DOI: 10.1002/ejoc.201100329

Selective Colorimetric Detection of Hg^{2+} and Mg^{2+} with Crown Ether Substituted *N*-Aryl-9-aminobenzo[*b*]quinolizinium Derivatives

Maoqun Tian[a] and Heiko Ihmels*[a]

Dedicated to Professor Siegfried Hünig on the occasion of his 90th birthday

Keywords: Absorption / Chemosensors / Heterocycles / Quinolizinium ions / Solvent effects

1,4-Dioxa-7,13-dithia-10-azacyclopentadecane ($AT_2$15C5) or 1,4,7,10-tetraoxa-13-azacyclopentadecane (A15C5) were attached as metal-ion-binding receptor units at the *ortho* or *para* positions of the 9-amino-*N*-phenylbenzo[*b*]quinolizinium chromophore. The addition of Hg^{2+} or Mg^{2+} to the *para* isomers of the $AT_2$15C5–quinolizinium or A15C5–quinolizinium conjugate, respectively, led to a blueshift of the absorption maxima of each compound because of the reduced donor ability of the complexed amino group. In contrast, the addition of Hg^{2+} to a solution of the *ortho*-$AT_2$15C5–quinolizinium conjugate in H_2O/MeOH mixtures induced a significant redshift (ca. 50 nm) of the absorption maximum and enabled the photometric discrimination between Hg^{2+} and competing thiophilic cations, such as Ag^+ or Pb^{2+}, because the latter, as well as other competing metal ions, did not induce such an effect. It is proposed that the Hg^{2+}-induced redshift originates from the complexation of Hg^{2+} by the thiaazacrown ether followed by deprotonation of the secondary 9-amino substituent of the aminobenzoquinolizinium unit. The resulting amide functionality increases the donor–acceptor interplay leading to the redshifted absorption and also coordinates to Hg^{2+} to form a lariat ether type complex. A similar effect was observed upon the addition of Mg^{2+} to the 9-amino-*N*-phenylbenzo[*b*]quinolizinium derivative with the A15C5 unit in the *ortho* position; however, this effect was only operative in aprotic solvents, e.g. CH_3CN, and with less than 1 mol-equiv. of Mg^{2+}.

Introduction

Metal cations are essential components in biological and ecological media,[1,2] and a deviation from the required concentration of each cation may induce harmful effects on the environment, namely, contamination and pollution, or on physiological systems, leading to serious diseases. Therefore, the development of sensitive and selective optical probes for cation detection has attracted much attention in recent years.[3] In particular, colorimetric probes allow straightforward and inexpensive cation detection, even without sophisticated equipment, because the color change may be observed by the naked eye. In general, a cation may be detected by the optical response from the probe caused by selective reaction or association, namely, the modulation of charge-transfer efficiency by cation complexation,[4] cation-induced aggregation or disaggregation of the probe molecules,[5] *cis*/*trans* isomerization upon intramolecular chelation,[6] irreversible chemical transformation of chemodosimeters,[7] or the analyte-induced change of a complexing site in a host–guest assembly based on keto–enol tautomerism.[8]

Considering the hazardous effects of mercury in biological and ecological systems,[9] we have focused our attention on the photometric and fluorimetric detection of Hg^{2+} ions.[10] For this purpose, we developed the probe molecules **1a** and **2**, in which an Hg^{2+}-selective thiaazacrown ether receptor was integrated into a 9-aminobenzo[*b*]quinolizinium (also known as 9-aminoacridizinium) chromophore. The latter unit was chosen, because the donor–acceptor interplay, and thus the absorption or emission properties, can be modified by changing the donor properties of the exocyclic amino functionality by Hg^{2+} complexation. Moreover, the benzo[*b*]quinolizinium ion is water-soluble, which facilitates studies in aqueous solutions, as required for the detection of physiologically relevant analytes. Indeed, the derivatives **1a** and **2** may be used for the fluorimetric detection of Hg^{2+}; however, Ag^+ ions interfere with the detection, because they bind to the receptor unit as well. Herein, we present the selective colorimetric detection of Hg^{2+} with probe **1a** without interference of Ag^+. For comparison, and to evaluate the generality of this approach, the crown ether unit was modified in **1b** such that it was selective towards the alkaline earth metal cation Mg^{2+}. Moreover, the influence of the substitution pattern on the colorimetric cation detection was examined with isomers that had receptor units attached at the *para* position of the phenyl substituent.

[a] Universität Siegen, Organische Chemie II,
Adolf-Reichwein-Strasse 2, 57068 Siegen, Germany
Fax: +49-271-740-4052
E-mail: ihmels@chemie.uni-siegen.de

Supporting information for this article is available on the WWW under http://dx.doi.org/10.1002/ejoc.201100329.

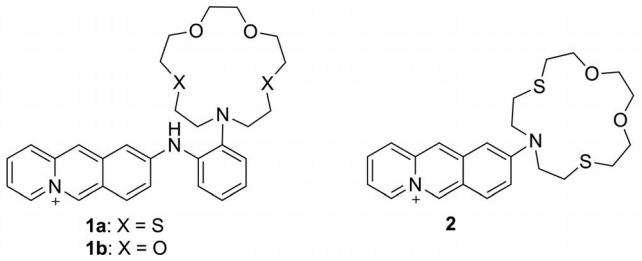

Results

The 9-amino-*N*-arylbenzo[*b*]quinolizinium derivatives **1a**–**d** were synthesized according to modified literature procedures (Scheme 1).[11] Thus, nucleophilic substitution reactions of the fluoronitrobenzene derivatives **3a** or **3b** with the azacrown ether derivatives 1,4-dioxa-7,13-dithia-10-azacyclopentadecane ($AT_2$15C5-H) and 1,4,7,10-tetraoxa-13-azacyclopentadecane (A15C5-H) followed by the reduction of the nitro functionality gave the aniline derivatives **5a**–**d** in 54–98% yield, respectively. The subsequent nucleophilic substitution reaction of 9-fluorobenzo[*b*]quinolizinium bromide with **5a**–**d** produced the corresponding crown ether derivatives **1a**–**d** in 10–46% yields. The structures of the new compounds **1b**, **1c**, **1d**, **4c**, and **5c** were confirmed by ^{1}H and ^{13}C NMR spectroscopic analysis, mass spectrometry, and elemental analysis data.

The spectrophotometric titrations of the *para*-substituted crown ether derivatives **1c** and **1d** with Hg^{2+} (in MeOH) and Mg^{2+} (in MeCN) led to a decrease of the long-wavelength absorption band and to an increase of the intensity of the absorption-band maximum at about 400 nm, along with a slight blueshift (Figure 1A and B). In addition, isosbestic points were formed during the titration. The binding isotherms were fitted to a 1:1 binding stoichiometry with binding constants of 2.7×10^4 M^{-1} for **1c**–Hg^{2+} and 1.9×10^3 M^{-1} for **1d**–Mg^{2+} (cf. Figure S1 in the Supporting Information).

Recently, we have observed that derivative **1a**, which carries an *ortho*-thiaazacrown ether substituent, has a different optical response to the complexation of Hg^{2+} than isomer **1c**,[10a] because the long-wavelength absorption band between 430 and 500 nm increases slightly upon addition of Hg^{2+} in aqueous buffer solution. During studies of this phenomenon in different solvents, we discovered a notable influence of the composition of methanol/water mixtures on the photometric titrations. Although the absorption spectra of **1a** are essentially identical in each of the solvent mixtures, a significant difference of the development of the long-wavelength absorption band upon the addition of Hg^{2+} was observed in solutions with different water/methanol ratios (Figure 1C and D, cf. Figure S2 in the Supporting Information). Specifically, with an increasing content of methanol the decrease of the absorption band at 392 nm and the increase of the band at 450 nm are more pronounced, as demonstrated by the superposition of the absorption spectra of the **1a**–Hg^{2+} complexes in different solvent mixtures (Figure 1D). The binding constants of **1a** with Hg^{2+}, as deduced from the corresponding binding isotherms, were essentially the same within the error margin in methanol/water mixtures, that is, $K = 1.0 \times 10^5$, 1.6×10^5 and 1.2×10^5 M^{-1} (cf. Figure S2 in the Supporting Information). In pure methanol, the binding constant is larger by one order of magnitude (1.0×10^6 M^{-1}). The 1:1 stoichiometry of the **1a**–Hg^{2+} complex in buffer/methanol (1:3) was confirmed by a Job plot (cf. Figure S3 in the Supporting Information). Notably, the change of absorption of **1a** upon the addition of Hg^{2+} is recognized by the naked eye as a color change from yellow to red (Figure 2). The plot of the ratio of the absorption at 520 and 404 nm, A_{520}/A_{404}, versus concentration of Hg^{2+} is linear over a large range and may be used for the quantitative detection of Hg^{2+} ions (cf. Figure S4 in the Supporting Information). The limit of detection is 0.10 μM, with a linear range from 0 to 75 μM. Moreover, the redshift upon cation addition is highly selec-

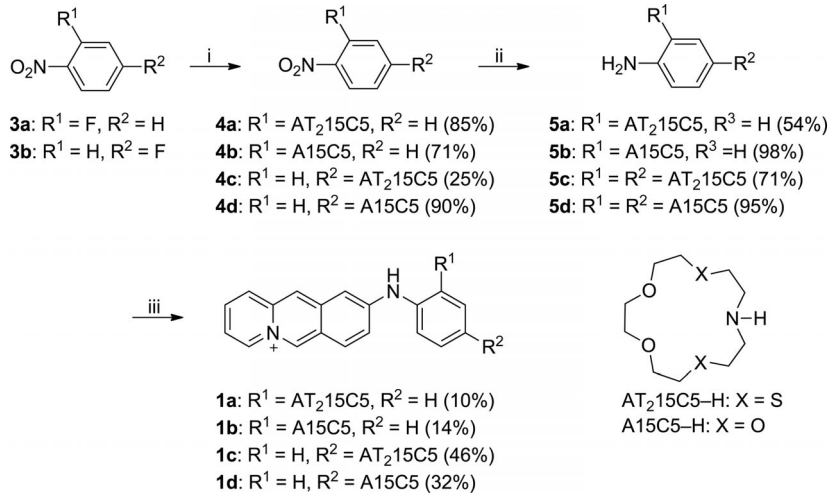

Scheme 1. Synthesis of 9-amino-*N*-arylbenzo[*b*]quinolizinium derivatives **1a**–**d**. Reagents and conditions: (i) $AT_2$15C5-H or A15C5-H, Cs_2CO_3, 60 °C 12 h (**4a**–**b**), or Cs_2CO_3, DMF, 100 °C, 24 h (**4c**–**d**); (ii) $SnCl_2$, EtOH, reflux, 3 h (**5a** and **5c**) or Pd/C H_2, EtOAc, room temp., 12–24 h (**5b** and **5d**); (iii) 9-fluorobenzo[*b*]quinolizinium bromide, EtOH, reflux, 12–72 h.

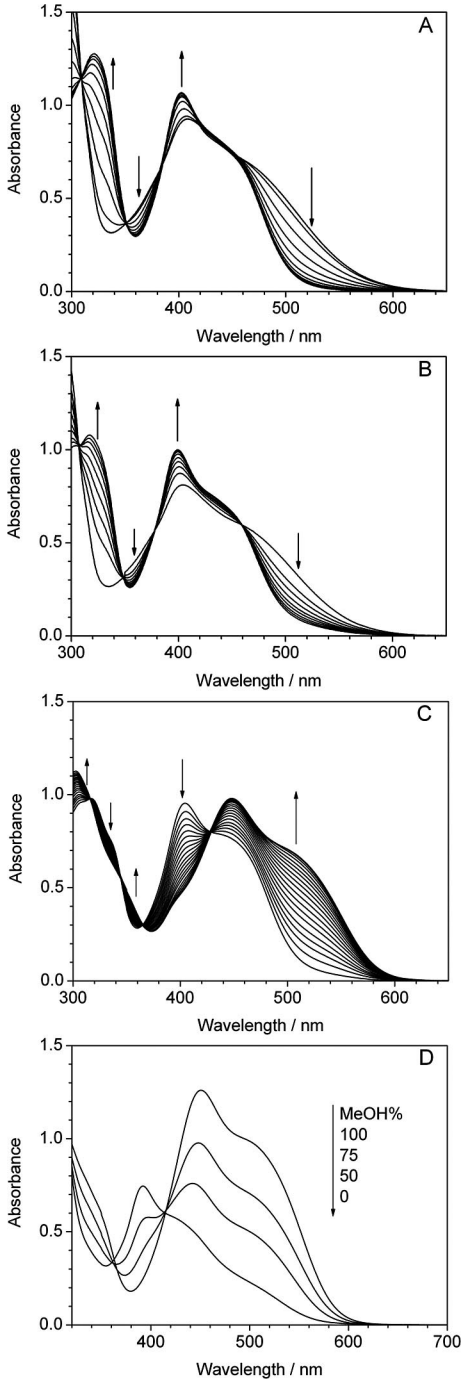

Figure 1. (A) Spectrophotometric titrations of **1c** (50 μM) with $Hg(OAc)_2$ (0–0.22 mM) in MeOH. (B) Spectrophotometric titrations of **1d** (50 μM) with $Mg(ClO_4)_2$ (0–2.2 mM) in MeCN. (C) Spectrophotometric titrations of **1a** (50 μM) with $Hg(OAc)_2$ (0–0.13 mM) in HEPES buffer (75% MeOH). (D) Absorption spectra of the **1a**–Hg^{2+} complex in aqueous HEPES buffer solution with various methanol contents.

tive, because it is only induced by Hg^{2+}, but not by the potentially competing[12] transition-metal cations, such as Ag^+, Zn^{2+}, Cd^{2+}, Co^{2+}, Ni^{2+}, Cr^{3+}, Cu^{2+}, Pb^{2+}, Fe^{3+}, and Fe^{2+} (Figure 2). Only the addition of Ag^+ induced a blue-shift of the absorption, but with almost no clear color change.

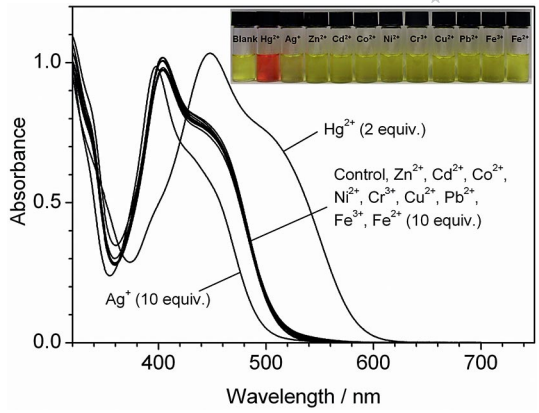

Figure 2. Absorption of **1a** (50 μM) in HEPES buffer/methanol (1:3, 25 mM, pH = 7.0) in the presence of Hg^{2+} (2.0 equiv.), Ag^+, Zn^{2+}, Cd^{2+}, Co^{2+}, Ni^{2+}, Cr^{3+}, Cu^{2+}, Pb^{2+}, Fe^{3+}, and Fe^{2+} (10 equiv.). Inset: picture of **1a** in the presence of selected metal cations.

Complex formation between the benzo[*b*]quinolizinium derivative **1a** and Hg^{2+} was also examined by ^1H NMR spectroscopic analysis (Figure 3). In CD_3OD, most proton signals of the benzo[*b*]quinolizinium part are shifted to higher field ($\Delta\delta$ = 0.1–0.5 ppm) upon the addition of Hg^{2+} (1 mol-equiv.). In contrast, a low-field shift of $\Delta\delta$ = 0.1 ppm was observed for the proton signal of 8-H (Figure 3A and B). The signals of the phenyl protons only showed slight changes ($\Delta\delta$ = 0.05–0.10 ppm) of the chemical shifts upon the addition of Hg^{2+} ions. In D_2O, most aromatic proton signals of **1a** shift to lower field upon the addition of Hg^{2+}, whereas the signal of 10-H was high-field-shifted by $\Delta\delta$ = 0.25 ppm (Figure 3C and D). In both cases, the ^1H NMR signals of the crown ether units are significantly broadened

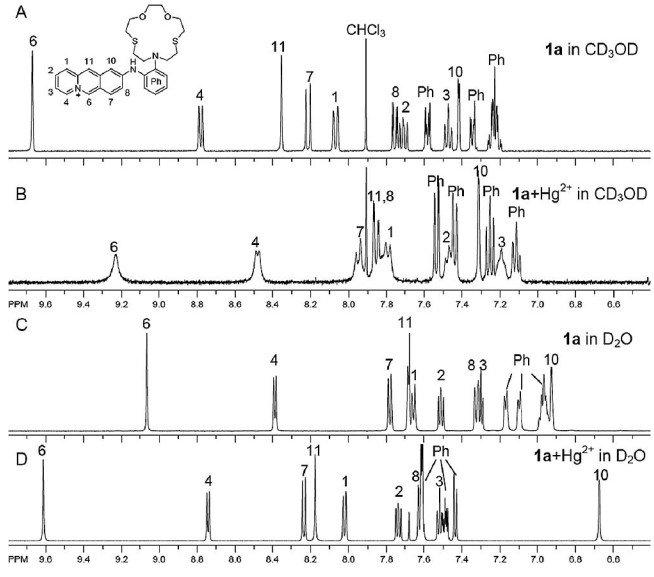

Figure 3. ^1H NMR spectra of **1a** in CD_3OD (A) and D_2O (C) and in the presence of Hg^{2+} (1 mol-equiv.) in CD_3OD (B) and D_2O (D). Chloroform is the lattice solvent in the crystal of compound **1a** after recrystallization from $CHCl_3$/EtOAc.

in the presence of Hg^{2+} (data not shown), which is a characteristic indication of complex formation.

The absorption properties of the benzo[*b*]quinolizinium derivative **1a** also change upon protonation (Figure 4). The titration of aqueous hydrochloric acid into a solution of **1a** in buffer solution led to a blueshift of the long-wavelength absorption maximum from 400 to 385 nm, along with a decrease of the broad long-wavelength absorption shoulder. A plot of the absorption at 440 nm versus the pH of the solution fits appropriately to an acid–base equilibrium with a pK_a of 3.0 (inset in Figure 4).

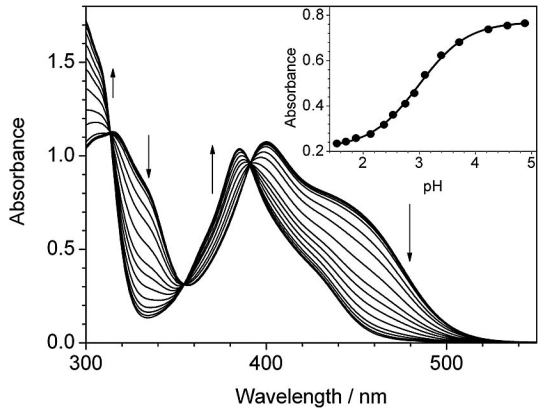

Figure 4. Spectrophotometric titration of aqueous HCl (2 M) into a solution of **1a** (c = 50 μM) in Britton–Robinson buffer (pH = 1.5–4.9). The arrows indicate the changes of the bands upon acidification. Inset: plot of the absorption at 440 nm versus pH of the solution; numerical fit calculated for pK_a = 3.0.

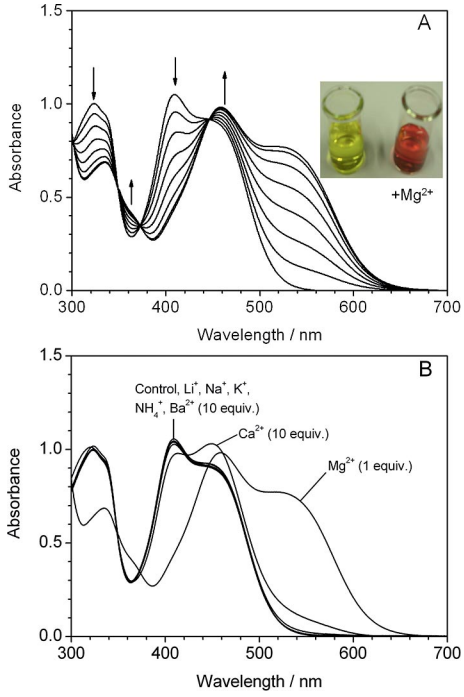

Figure 5. (A) Spectrophotometric titration of $Mg(ClO_4)_2$ (0–70 μM) into a solution of **1b** (50 μM) in MeCN. Inset: image of **1b** in the absence (left) and in the presence of Mg^{2+} (right). (B) Absorption of **1b** (50 μM) in acetonitrile in the presence of Mg^{2+} (1.0 equiv.), Li^+, Na^+, K^+, NH_4^+, Mg^{2+}, Ca^{2+}, and Ba^{2+} (10 equiv.).

To assess whether the *ortho* substitution of an appropriate receptor unit at the phenyl group of 9-amino-*N*-phenylbenzo[*b*]quinolizinium derivatives may be employed in general for cation detection, the absorption of the azacrown-substituted derivative **1b** was determined in acetonitrile in the presence of the perchlorate salts of potentially competing cations:[12] NH_4^+, Li^+, Na^+, K^+, Mg^{2+}, Ca^{2+}, or Ba^{2+} (Figure 5). Notably, only the addition of Mg^{2+} induced a large redshift of the long-wavelength absorption, resulting in a color change of the solution from yellow to red. A numerical fit of the titration isotherm to a 1:1 binding stoichiometry gave a binding constant of $K = 6.5 \times 10^5$ M^{-1} (cf. Figure S6 in the Supporting Information). Among the other cations tested only Ca^{2+} induced a slight redshift of the absorption of **1b**. Notably, the addition of excess Mg^{2+} (c > 0.3 mM) resulted in a decrease of the absorption band at 450–600 nm, along with a significant enhancement of fluorescence by a factor of 1800 (Figure 6), which was also selective for Mg^{2+}.

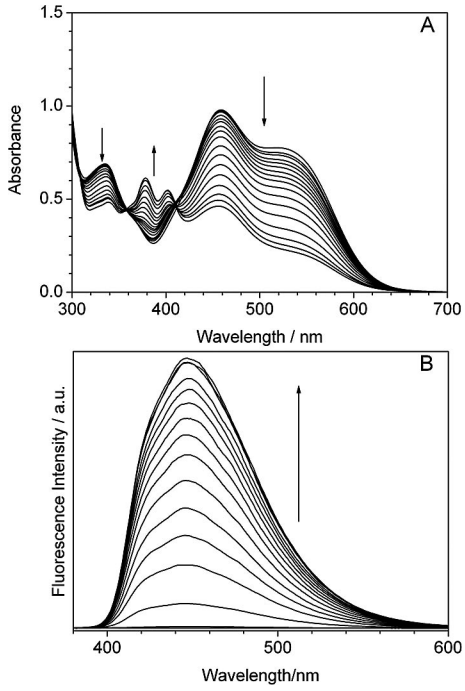

Figure 6. (A) Spectrophotometric titration of **1b** (50 μM) with Mg^{2+} (70 μM–10 mM) in MeCN. (B) Spectrofluorimetric titration of Mg^{2+} (0.3 mM–15 mM) into a solution of **1b** (10 μM) in MeCN; λ_{ex} = 358 nm.

Discussion

In general, it was observed that all crown ether–benzo[*b*]quinolizinium conjugates changed their absorption properties upon the addition of a metal cation that bound to the crown ether receptor. However, depending on the substitution pattern (*ortho* vs. *para* substitution of the crown ether) and on the solvent, different trends could be distinguished. In the case of the *para*-substituted derivatives **1c** and **1d**, the changes of the absorption properties are charac-

teristic of conjugated donor–acceptor chromophores, the donor group of which binds to a metal cation.[4] Specifically, complexation of the metal ions by the azacrown ether leads to a change of the substituent effect of the phenylenediamine unit, because the complexed azacrown substituent resembles the chloro substituent.[13] As a result, the donor–acceptor interplay with the benzo[*b*]quinolizinium unit is very weak compared with the uncomplexed compounds **1c** or **1d**, leading to a blueshift of the absorption bands and to the disappearance of the low-energy charge-transfer band at $\lambda > 500$ nm. However, because of the relatively small blueshift of the absorption, which is hardly noticed by the naked eye, these compounds may not be considered ideal probes for colorimetric cation detection. The titration of Hg^{2+} into the isomeric thiaazacrown ether **1a** in water also induced a blueshift of the absorption maximum, thus indicating the participation of the amino group of the azacrown receptor in the complexation of Hg^{2+}. The amine–Hg^{2+} interaction was further confirmed by the ^1H NMR spectroscopic analysis (Figure 3C and D), namely, the low-field shift of almost all proton signals, including those of the phenylenediamine unit, clearly indicated the reduced donor strength of the amino functionality upon complexation. Moreover, this assumption is in agreement with the photometric titration of acid to **1a**, because the protonation of the amino function of the crown ether also leads to a blueshift of the absorption maximum (Figure 4). It can be excluded that the amino group at the 9-position of the benzo[*b*]quinolizinium unit is protonated, because it has been shown already that this position is only very weakly alkaline in 9-amino-*N*-arylbenzo[*b*]quinolizinium derivatives.[14] Also, the pK_a of 3.0 is comparable to those of similar azacrown receptors.[15]

Surprisingly, an additional redshifted absorption shoulder developed along with the blueshift of the maximum upon the addition of Hg^{2+} to **1a** in water. The former cannot be readily explained by the complexation of the crown ether amino group with Hg^{2+}. Remarkably, with increasing methanol content in the solution, the long-wavelength shoulder develops into an absorption maximum at the expense of the blueshifted low-wavelength absorption band (Figure 1D); most likely as a result of a more pronounced donor–acceptor interaction. These observations indicate two different absorbing species after complexation of Hg^{2+}. The significant redshift upon addition of Hg^{2+}, as well as the impact of the solvent on this effect, are apparently a consequence of the *ortho*-substitution pattern in **1a**, because this effect was not observed for the *para* isomer **1c**. A helpful comparison for this situation may be provided by metal complexes of the so-called *ortho*-Wurster's crown **6**, the *ortho*-dimethylamino group of which coordinates in a lariat ether type complexation towards a bound metal cation.[16] In contrast, the oxidation of the phenylenediamines induces a rotation of the pendant amino group away from the crown fragment because of the repulsive electrostatic interactions between the ligand radical cation and the cationic guest. These specific structural conditions lead to electrochemical properties of **6** that are significantly different from those of the isomeric *para*-Wurster's crown. Based on these observations, we propose that ligand **1a** and Hg^{2+} also form two complexes with distinctly different structures. In water, a similar situation occurs as that in the oxidized Wurster's crown, that is, the complex formation introduces additional positive charge, and to avoid electrostatic repulsion the complexed crown unit and the benzo[*b*]quinolizinium unit rotate away from each other to achieve a conformation in which the secondary 9-amino group is conjugated to the phenyl ring to compensate for the positive polarization. At the same time, this arrangement reduces the donor–acceptor interplay between the NH group and the benzo[*b*]-quinolizinium unit, leading to the observed blueshift of the absorption (see above). With increasing methanol content of the solution, however, the accumulated charge in the complex **1a**–Hg is less stabilized by the solvent than in pure water. In this case, the overall positive charge of the complex is reduced by deprotonation of the NH functionality, with the counteranion, buffer components, or the solvent acting as the proton acceptor, which also enables additional stabilization by an intramolecular complexation of the newly formed amide functionality with the Hg^{2+} ion (Scheme 2). The deprotonation of the amino substituent increases its π-donor property and leads to the redshift of the absorption maximum (Figure 1C) and to the high-field shift of the ^1H NMR signals of the benzo[*b*]quinolizinium (Figure 3). Such a deprotonation reaction of amino or amido

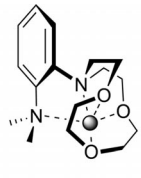

6; ● = Li^+

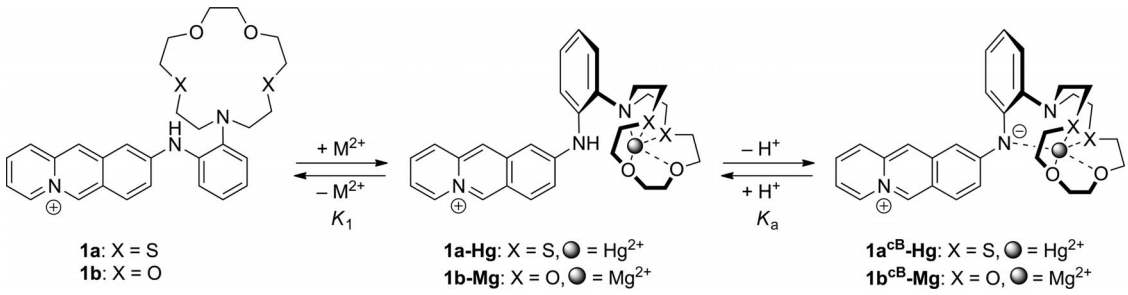

Scheme 2. Proposed structures of the **1a**–Hg^{2+} complex (cB = conjugate base).

substituents in water/alcohol, as induced by metal-ion complexation, is a well-known reaction of donor–acceptor-type dyes that carry a receptor unit close to the NH functionality.[17] In the latter cases, the deprotonation also leads to a significant redshift of the absorption maxima because of the increased donor ability of the deprotonated amine. Further experimental support for the formation of **1a**^{cB}–Hg was provided by photometric titrations. Thus, it was shown that the addition of acid to the complex between **1a** and Hg^{2+} in a buffer solution induced a decrease of the long-wavelength absorption band and an increase of the absorption maximum at 390 nm (cf. Figure S5 in the Supporting Information), resembling the absorption of **1c**–Hg^{2+}. In addition, the contribution of the intramolecular $N^{-}\cdots Hg^{2+}$ complexation to the overall stabilization of the complex is indicated by the observation that such a deprotonation does not take place in the complex of the *para* isomer **1c** with Hg^{2+}.

It may be assumed that the tertiary amino group of the azacrown ether in **1a**^{cB}–Hg is not, or only weakly, coordinated to the Hg^{2+} ion, as shown theoretically for aza-15-crown ether complexes.[18] This decomplexation of the nitrogen ligand would explain the small changes of the ^{1}H NMR signals of the *o*-phenylenediamine upon complexation, because the tertiary amino group of the azacrown ether is conjugated with the phenyl ring, acting as a π-donor, whereas the deprotonated amine is twisted towards the plane of the benzene ring, so that it has solely σ-acceptor properties. This situation resembles that in *o*-phenylenediamine in which one amino group is also decoupled from π-conjugation.[19]

It should be stressed that the determined apparent binding constant, K, between **1a** and Hg^{2+} is the combination of the complex association constant, K_1, and the acidity constant, K_a, of the two-step equilibrium between **1a**, **1a**–Hg, and **1a**^{cB}–Hg (Scheme 2). Although these binding constants were not further dissected, it is apparent that the affinity of the crown ether ligand towards Hg^{2+} is sufficient to enable the selective detection of this ion with the probe molecule **1a**. Interestingly, the isosbestic points are maintained during titration, which is somewhat unusual, because it is commonly assumed that an isosbestic point is formed during spectrophotometric titrations if one starting material is converted exclusively into one single product quantitatively. In contrast, it has been demonstrated that isosbestic points may even be observed if multiple products are formed, as long as the fractional yield of the absorbing products is constant.[20] By considering the constant pH during the titration of Hg^{2+} with **1a**, it may be assumed that in this case fractional conversion to **1a**–Hg and **1a**^{cB}–Hg is constant during the titration, thus leading to the isosbestic points.

The high affinity of Hg^{2+} and Ag^{+} for the crown ether unit in **1a**[21] causes the selective change of the absorption of **1a**. Nevertheless, the lower charge of Ag^{+}, compared with Hg^{2+}, leads to less positive charge in a complex with **1a**, so that deprotonation, such as that in **1a**–Hg, does not take place. Also, chelation in **1a**–Ag by the deprotonated NH functionality, if formed at all, may be unfavorable due to the larger size of Ag^{+}. Therefore, the addition of Ag^{+} to **1a** results in an exclusive blueshift of the absorption. ^{1}H NMR spectroscopic analysis provided further evidence for different structures of the complexes **1a**–Hg and **1a**–Ag in MeOD: In contrast to the spectra obtained for the complex **1a**–Hg (Figure 3), the proton signals of **1a** shifted only slightly to lower field upon the addition of Ag^{+} (cf. Figure S18 in the Supporting Information). In particular, the latter effect was most pronounced for the crown ether fragment, whereas the signals of the aromatic unit remained essentially unchanged, indicating that there was no significant complexation by the nitrogen atom of the azacrown part.[22]

Such as in the case of **1a** and Hg^{2+}, the addition of Mg^{2+} to derivative **1b** resulted in the same effect. Therefore, it may be concluded that a similar equilibrium between **1b**, **1b**–Mg, and **1b**^{cB}–Mg is established (Scheme 2). The selectivity of this effect for Mg^{2+} may be attributed to the participation of the lariat-type amide group to form, in addition to complexation with the crown ether, an appropriate cavity size for Mg^{2+} binding (Scheme 2).[23] However, when the concentration of Mg^{2+} exceeds that of **1b**, the redshifted absorption decreases, whereas a new blueshifted band develops. Presumably, at higher Mg^{2+}/**1b** ratios, an additional Mg^{2+} ion binds to the complex **1b**^{cB}–Mg, most likely at the amide functionality. The redistribution of amide ligands in Mg complexes has been shown to operate in solution, and the driving force for this process may be the strong N–Mg interaction.[24] The blueshift of the absorption and emission maxima indicates the reduced donor ability of the nitrogen atom in this complex, which is likely to result from steric strain and a twist of the benzo[*b*]quinolizinium unit about the C–N bond such that conjugation with the nitrogen atom at C-9 is significantly reduced. The increased emission intensity may be the result of reduced conformational flexibility of the complex, because it has been shown that the low emission quantum yield of 9-amino-*N*-arylbenzo[*b*]quinolizinium derivatives is mainly caused by the torsional relaxation.[14] Unfortunately, the large excess of Mg^{2+} required to induce this light-up effect restricts the application of this effect for sensitive fluorimetric detection of Mg^{2+}.

Conclusions

A tool for the selective colorimetric detection of cations based on complexation-induced deprotonation and subsequent lariat-type chelation was developed. Specifically, benzo[*b*]quinolizinium derivative **1a** represents one of the few chemosensors that allows discrimination between Hg^{2+} and competing thiophilic cations, such as Ag^{+} or Pb^{2+} ions, which often interfere with Hg^{2+} detection.[25] At the same time, derivative **1b** enables the selective colorimetric detection of Mg^{2+}. Furthermore, the variation of the receptor or chromophore unit may offer the opportunity to extend this approach for the optical detection of other biologically or ecologically relevant cations.

Experimental Section

General Instrumentation and Materials: The melting points were measured with a melting point apparatus (Büchi 510 K). Mass spectra (ESI in the positive-ion mode, source voltage 6 kV) were recorded with a Finnigan LCQ Deca instrument; only *m*/*z* values in the range of 100–2000 units were analyzed. NMR spectra were measured with Bruker Avance 400 (^{1}H: 400 MHz; ^{13}C: 100 MHz) and Varian NMR System 600 (^{1}H: 600 MHz; ^{13}C: 150 MHz) spectrometers at 20 °C; chemical shifts are given in ppm (δ) values (internal standards TMS for ^{1}H and ^{13}C NMR spectra). ^{1}H NMR chemical shifts of **1a** in the absence and presence of Hg^{2+} are given relative to solvent signals: δ = 3.31 ppm for CHD_2OD, δ = 4.79 ppm for HDO. Elemental microanalyses of all new compounds were performed with a HEKAtech EuroEA combustion analyzer by H. Bodenstedt (Institut für Organische Chemie, Universität Siegen). Absorption spectra were recorded with a Varian Cary 100 double-beam spectrophotometer; fluorescence emission spectra were recorded with a Varian Cary Eclipse fluorescence spectrometer. The pH of aqueous solutions was measured with a calibrated pH meter (Qph 70, VWR). TLC analysis of benzo[*b*]-quinolizinium derivatives was performed on silica-gel sheets (Macherey–Nagel Polygram Sil G/UV254), eluent: $CHCl_3$/MeOH (90:10, v/v). All commercially available chemicals were reagent grade and used without further purification. Diethyl ether and THF were distilled from sodium wire; DMF, DMSO, and dichloromethane were dried with calcium hydride and vacuum-distilled prior to use; ethanol was purified by rectification. Other solvents were analytical or HPLC grade and used without further purification. Distilled water was used for experiments. The term "purified water" refers to e-Pure™ water (resistivity 18 MΩcm^{-1}). 9-Fluorobenzo[*b*]quinolizinium bromide and $AT_2$15C5-H were prepared according to literature procedures.[26] For the identification of known compounds, the spectroscopic data were compared with the literature data. Metal cations were employed as the corresponding perchlorate salts, except for photometric Hg^{2+} titrations, which were performed with $Hg(OAc)_2$. Control experiments showed no difference in the optical response with different counterions, $Hg(ClO_4)_2$ versus $Hg(OAc)_2$.

General Procedure for the Reaction of 1-Fluoro-2-nitrobenzene with the Azacrown Ether $AT_2$15C5-H or A15C5-H: A suspension of **3a** (4.12 g, 29.2 mmol), Cs_2CO_3 (2.98 g, 9.14 mmol), and the corresponding azacrown ether (3.80 mmol) was stirred under nitrogen at 60 °C for 72 h. After cooling the reaction mixture to room temp., water (100 mL) was added, and the aqueous layers were extracted with chloroform (3 × 100 mL). The combined organic layers were washed with brine (100 mL) and dried with $MgSO_4$. After evaporation of the solvent in vacuo, the product was isolated by column chromatography (SiO_2; dichloromethane/hexane, 1:1).

***N*-(2-Nitrophenyl)-1,4-dioxa-7,13-dithia-10-azacyclopentadecane (4a):** Yield 1.20 g (85%), orange oil. ^{1}H NMR (400 MHz, $CDCl_3$): δ = 2.72 (t, ^3J = 5 Hz, 4 H, CH_2), 2.84–2.88 (m, 4 H, CH_2), 3.39–3.41 (m, 4 H, CH_2), 3.67 (s, 4 H, CH_2), 3.77 (t, ^3J = 5 Hz, 4 H, CH_2), 6.95–6.99 (m, 1 H, CH_{ar}), 7.18 (dd, ^4J = 1, ^4J = 1 Hz, 1 H, CH_{ar}), 7.39–7.44 (m, 1 H, CH_{ar}), 7.67 (dd, ^4J = 1, ^4J = 1 Hz, 1 H, CH_{ar}) ppm.[10a]

***N*-(2-Nitrophenyl)-1,4,7,10-tetraoxa-13-azacyclopentadecane (4b):** Yield 917 mg (71%), orange oil. ^{1}H NMR (400 MHz, $CDCl_3$): δ = 3.44 (t, ^3J = 6 Hz, 4 H, CH_2), 3.59–3.70 (m, 16 H, CH_2), 6.89–6.94 (m, 1 H, CH_{ar}), 7.33 (dd, ^3J = 8, ^4J = 1 Hz, 1 H, CH_{ar}), 7.37–7.43 (m, 1 H, CH_{ar}), 7.63 (dd, ^3J = 8, ^4J = 2 Hz, 1 H, CH_{ar}) ppm.[16]

General Procedure for the Reaction of 1-Fluoro-4-nitrobenzene with the Azacrown Ether $AT_2$15C5-H or A15C5-H: A suspension of **3b** (13.3 g, 94.3 mmol), the corresponding azacrown ether (13.3 mmol), and Cs_2CO_3 (5.66 g, 16.0 mmol) in DMF (35 mL) was stirred under nitrogen at 100 °C for 24 h. After cooling to room temp., the reaction mixture was concentrated to dryness, and water (200 mL) was added to the residue. The mixture was extracted with CH_2Cl_2 (4 × 100 mL). The combined organic layers were washed by brine and dried with Na_2SO_4. After evaporation of the solvent, the product was purified by column chromatography (SiO_2; EtOAc/hexane, 1:2) and subsequent recrystallization from EtOH.

***N*-(4-Nitrophenyl)-1,4-dioxa-7,13-dithia-10-azacyclopentadecane (4c):** Yield 1.22 g (25%), yellow powder; m.p. 129–132 °C. ^{1}H NMR (400 MHz, $CDCl_3$): δ = 2.78 (t, ^3J = 5 Hz, 4 H, CH_2), 2.91 (t, ^3J = 8 Hz, 4 H, CH_2), 3.67 (s, 4 H, CH_2), 3.75 (t, ^3J = 8 Hz, 4 H, CH_2), 3.82 (t, ^3J = 5 Hz, 4 H, CH_2), 6.59 (d, ^3J = 9 Hz, 2 H, CH_{ar}), 8.12 (d, ^3J = 9 Hz, 2 H, CH_{ar}) ppm. ^{13}C NMR (400 MHz, $CDCl_3$): δ = 29.2 (2 CH_2), 31.5 (2 CH_2), 52.1 (2 CH_2), 70.6 (2 CH_2), 74.4 (2 CH_2), 110.4 (2 CH_{ar}), 126.4 (2 CH_{ar}), 137.1 (C_q), 151.7 (C_q) ppm. MS (ESI$^+$): *m*/*z* (%) = 373 (20) $[M + H]^+$. $C_{16}H_{24}N_2O_4S_2$ (372.50): calcd. C 51.59, H 6.49, N 7.52, S 17.22; found C 51.62, H 6.49, N 7.51, S 17.23.

***N*-(4-Nitrophenyl)-1,4,7,10-tetraoxa-13-azacyclopentadecane (4d):** Yield 4.07 g (90%), yellow oil. ^{1}H NMR (400 MHz, $CDCl_3$): δ = 3.60–3.72 (m, 16 H, CH_2), 3.79 (t, ^3J = 4 Hz, 4 H, CH_2), 6.59–6.66 (m, 2 H, CH_{ar}), 8.07–8.14 (m, 2 H, CH_{ar}) ppm.[16]

General Procedure for the Reduction of *N*-(Nitrophenyl)-1,4,7,10-tetraoxa-13-azacyclopentadecane: A suspension of **4b** or **4d** (2.00 mmol) and 10% Pd/C (0.2 mmol) in ethyl acetate (10 mL) was stirred under hydrogen at room temp. for 24 h. The solid catalyst was removed by filtration and rinsed with ethyl acetate. The filtrate was concentrated under reduced pressure to yield the desired product.

***N*-(2-Aminophenyl)-1,4,7,10-tetraoxa-13-azacyclopentadecane (5b):** Yield 608 mg (98%), colorless oil. ^{1}H NMR (400 MHz, $CDCl_3$): δ = 3.17 (t, ^3J = 5 Hz, 4 H, CH_2), 3.49 (t, ^3J = 5 Hz, 4 H, CH_2), 3.60–3.64 (m, 4 H, CH_2), 3.66–3.72 (m, 8 H, CH_2), 6.63–6.72 (m, 2 H, CH_{ar}), 6.90–6.96 (m, 1 H, CH_{ar}), 7.08 (dd, ^3J = 8, ^4J = 1 Hz, 1 H, CH_{ar}) ppm.[16]

***N*-(4-Aminophenyl)-1,4,7,10-tetraoxa-13-azacyclopentadecane (5d):** Yield 590 mg (95%), colorless oil. ^{1}H NMR (400 MHz, $CDCl_3$): δ = 3.50 (t, ^3J = 6 Hz, 4 H, CH_2), 3.61–3.69 (m, 12 H, CH_2), 3.72 (t, ^3J = 6 Hz, 4 H, CH_2), 6.53–6.59 (m, 2 H, CH_{ar}), 6.61–6.66 (m, 2 H, CH_{ar}) ppm.[16]

General Procedure for the Reduction of *N*-(Nitrophenyl)-1,4-dioxa-7,13-dithia-10-azacyclopentadecane: A suspension of **4a** or **4c** (3.22 mmol) and $SnCl_2 \cdot H_2O$ (4.28 g, 19.0 mmol) in ethanol (40 mL) was stirred under nitrogen at 90 °C for 3 h. After cooling the reaction mixture to room temp., the solvent was evaporated in vacuo, and ethyl acetate (150 mL) was added. An aqueous solution of Na_2CO_3 (5%) was added to adjust the pH to 8. The aqueous solution was extracted with ethyl acetate (3 × 100 mL), and the combined organic layers were washed with brine (100 mL) and dried with $MgSO_4$. The solvent was evaporated in vacuo. The product was obtained by recrystallization from ethyl acetate/hexane.

***N*-(2-Aminophenyl)-1,4-dioxa-7,13-dithia-10-azacyclopentadecane (5a):** Yield 596 mg (54%), orange needles; m.p. 101–103 °C. ^{1}H NMR (400 MHz, $CDCl_3$): δ = 2.75–2.81 (m, 8 H, CH_2), 3.18–3.22 (m, 4 H, CH_2), 3.69 (s, 4 H, CH_2), 3.79 (t, ^3J = 6 Hz, 4 H, CH_2), 4.10–4.32 (br. s, 2 H, NH_2), 6.69–6.72 (m, 2 H, CH_{ar}), 6.91–6.95 (m, 1 H, CH_{ar}), 7.04 (dd, ^4J = 1, ^4J = 1 Hz, 1 H, CH_{ar}) ppm.[10a]

***N*-(4-Aminophenyl)-1,4-dioxa-7,13-dithia-10-azacyclopentadecane (5c):** Yield 783 mg (71%), brown prisms; m.p. 94–97 °C. ^{1}H NMR

(400 MHz, $CDCl_3$): δ = 2.76 (t, ^3J = 5 Hz, 4 H, CH_2), 2.88 (t, ^3J = 8 Hz, 4 H, CH_2), 3.28 (br. s, 2 H, NH_2), 3.53 (t, ^3J = 8 Hz, 4 H, CH_2), 3.64 (s, 4 H, CH_2), 3.81 (t, ^3J = 5 Hz, 4 H, CH_2), 6.57 (d, ^3J = 8 Hz, 2 H, CH_{ar}), 6.65 (d, ^3J = 8 Hz, 2 H, CH_{ar}) ppm. ^{13}C NMR (400 MHz, $CDCl_3$): δ = 29.6 (2 CH_2), 31.0 (2 CH_2), 52.3 (2 CH_2), 70.7 (2 CH_2), 74.1 (2 CH_2), 114.2 (2 CH_{ar}), 117.0 (2 CH_{ar}), 137.0 (C_q), 140.6 (C_q) ppm. MS (ESI^+): *m/z* (%) = 343 (3) $[M + H]^+$. $C_{16}H_{26}N_2O_2S_2$ (342.52): calcd. C 56.11, H 7.65, N 8.18, S 18.72; found C 56. 23, H 7.67, N 8.08, S 18.72.

General Procedure for the Reaction of 9-Fluorobenzo[*b*]quinolizinium Bromide with Donor-Substituted Aniline Derivatives: A solution of 9-fluorobenzo[*b*]quinolizinium bromide (556 mg, 2.00 mmol) and the corresponding aniline derivative (2.00 mmol) in ethanol (5 mL) was stirred under reflux under nitrogen for 72 h. After cooling the reaction mixture to room temp., it was passed through an ion exchange resin (DOWEX®1 × 8 Cl^-). The product was purified by column chromatography (SiO_2; $CHCl_3$/MeOH, 10:1) and subsequent recrystallization from MeOH/ethyl acetate.

9-{[2-(1,4-Dioxa-7,13-dithia-10-azacyclopentadecyl)phenyl]amino}-benzo[*b*]quinolizinium Chloride (1a): Yield 116 mg (10%), orange-red needles; m.p. 240–241 °C. ^1H NMR (400 MHz, MeOD): δ = 2.68–2.75 (m, 8 H, CH_2), 3.25–3.28 (m, 4 H, CH_2), 3.64 (s, 4 H, CH_2), 3.72 (t, ^3J = 5 Hz, 4 H, CH_2), 7.19–7.24 (m, 2 H, Ph-H), 7.32–7.34 (m, 1 H, Ph-H), 7.41 (d, ^4J = 2 Hz, 1 H, 10-H), 7.45–7.47 (m, 1 H, 3-H), 7.56–7.58 (m, 1 H, Ph-H), 7.67–7.78 (m, 2 H, 2-H, 8-H), 7.91 (s, 1 H, $CHCl_3$), 8.06 (d, ^3J = 9 Hz, 1 H, 1-H), 8.20 (d, ^3J = 9 Hz, 1 H, 7-H), 8.35 (s, 1 H, 11-H), 8.77 (d, ^3J = 7 Hz, 1 H, 4-H), 9.67 (s, 1 H, 6-H) ppm.[10a]

9-{[2-(1,4,7,13-Tetraoxa-10-azacyclopentadecyl)phenyl]amino}-benzo[*b*]quinolizinium Perchlorate (1b): Fully characterized as the perchlorate salt, which was obtained by the addition of a saturated aqueous solution of sodium perchlorate to the solution of the chloride in methanol, and subsequent recrystallization of the precipitate from MeCN. Yield: 165 mg, 14%, orange prisms; m.p. 207–208 °C. ^1H NMR (400 MHz, CD_3OD): δ = 3.21 (t, ^3J = 5 Hz, 4 H, CH_2), 3.53 (t, ^3J = 5 Hz, 4 H, CH_2), 3.57–3.61 (m, 4 H, CH_2), 3.67–3.70 (m, 4 H, CH_2), 3.74 (s, 4 H, CH_2), 7.15–7.19 (m, 1 H, Ph-H), 7.21–7.26 (m, 1 H, Ph-H), 7.39 (dd, ^3J = 8, ^4J = 1 Hz, 1 H, Ph-H), 7.44–7.50 (m, 1 H, 3-H), 7.66–7.73 (m, 3 H, 2-H, 10-H, Ph-H), 7.99 (dd, ^3J = 9, ^4J = 2 Hz, 1 H, 1 H, 8-H), 8.08 (d, ^3J = 9 Hz, 1 H, 1-H), 8.17 (d, ^3J = 9 Hz, 1 H, 7-H), 8.37 (s, 1 H, 11-H), 8.79 (d, ^3J = 7 Hz, 1 H, 4-H), 9.65 (s, 1 H, 9-H) ppm. ^{13}C NMR (100 MHz, CD_3OD): δ = 55.7 (CH_2), 69.7 (CH_2), 71.1 (CH_2), 71.3 (CH_2), 71.4 (CH_2), 102.1 (CH_{ar}), 120.0 (CH_{ar}), 120.4 (CH_{ar}), 120.6 (CH_{ar}), 123.8 (C_q), 124.9 (CH_{ar}), 125.6 (CH_{ar}), 126.0 (CH_{ar}), 127.0 (CH_{ar}), 129.7 (CH_{ar}), 130.2 (CH_{ar}), 130.9 (CH_{ar}), 134.4 (CH_{ar}), 137.6 (C_q), 138.6 (CH_{ar}), 139.5 (C_q), 140.6 (C_q), 144.2 (C_q), 151.2 (C_q) ppm. MS (ESI^+): *m/z* (%) = 489 (100) $[M]^+$. $C_{29}H_{34}ClN_3O_8$ (588.05): calcd. C 59.23, H 5.83, N 7.15; found C 59.01, H 5.85, N 7.22.

9-{[4-(1,4-Dioxa-7,13-dithia-10-azacyclopentadecyl)phenyl]amino}-benzo[*b*]quinolizinium Chloride (1c): Yield 511 mg (46%), dark purple prisms; m.p. 240–244 °C. ^1H NMR (600 MHz, [D_6]DMSO): δ = 2.75 (t, ^3J = 5 Hz, 4 H, CH_2), 2.83 (t, ^3J = 8 Hz, 4 H, CH_2), 3.55–3.64 (m, 8 H, CH_2), 3.71 (t, ^3J = 5 Hz, 4 H, CH_2), 6.71 (d, ^3J = 9 Hz, 2 H, Ph-H), 7.13 (d, ^4J = 2 Hz, 1 H, 10-H), 7.23 (d, ^3J = 9 Hz, 2 H, Ph-H), 7.44–7.48 (m, 1 H, 3-H), 7.58 (dd, ^3J = 9, ^4J = 2 Hz, 1 H, 8-H), 7.66–7.70 (m, 1 H, 2-H), 7.99 (d, ^3J = 9 Hz, 1 H, 1-H), 8.16 (d, ^3J = 9 Hz, 1 H, 7-H), 8.36 (s, 1 H, 11-H), 8.82 (d, ^3J = 7 Hz, 1 H, 4-H), 9.69 (s, 1 H, NH), 9.81 (s, 1 H, 6-H) ppm. ^{13}C NMR (150 MHz, [D_6]DMSO): δ = 29.6 (2 CH_2), 31.0 (2 CH_2), 51.8 (2 CH_2), 70.5 (2 CH_2), 73.5 (2 CH_2), 98.9 (CH_{ar}), 112.7 (2 CH_{ar}), 118.0 (CH_{ar}), 119.0 (CH_{ar}) 121.5 (C_q), 125.0 (2 CH_{ar}), 125.8 (CH_{ar}), 125.8 (CH_{ar}),127.8 (C_q), 130.2 (CH_{ar}), 130.3 (CH_{ar}), 134.0 (CH_{ar}), 137.9 (C_q), 138.2 (CH_{ar}), 139.0 (C_q), 145.0 (C_q), 151.8 (C_q) ppm. MS (ESI^+): *m/z* (%) = 520 (100) $[M]^+$. $C_{16}H_{26}N_2O_2S_2{\cdot}H_2O$ (574.20): calcd. C 60.66, H 6.32, N 7.32, S 11.17; found C 60.47, H 6.38, N 7.30, S 11.19.

9-{[4-(1,4,7,13-Tetraoxa-10-azacyclopentadecyl)phenyl]amino}-benzo[*b*]quinolizinium Chloride (1d): Yield 335 mg (32%), purple needles; m.p. 246–248 °C. ^1H NMR (400 MHz, MeOD): δ = 3.71–3.56 (m, 16 H, CH_2), 3.78 (t, ^3J = 6 Hz, 4 H, CH_2), 6.74–6.81 (m, 2 H, Ph-H), 7.08 (d, ^4J = 2 Hz, 1 H, 10-H), 7.21–7.14 (m, 2 H, Ph-H), 7.40–7.33 (m, 1 H, 3-H), 7.51 (dd, ^3J = 9, ^4J = 2 Hz, 1 H, 8-H), 7.64–7.58 (m, 1 H, 2-H), 7.93 (d, ^3J = 9 Hz, 1 H, 1-H), 8.08 (d, ^3J = 9 Hz, 1 H, 7-H), 8.10 (s, 1 H, 11-H), 8.67 (d, ^3J = 7 Hz, 1 H, 4-H), 9.50 (s, 1 H, 6-H) ppm. ^{13}C NMR (100 MHz, CD_3OD): δ = 53.7 (CH_2), 70.0 (CH_2), 71.1 (CH_2), 71.4 (CH_2), 72.3 (CH_2), 100.3 (CH_{ar}), 113.5 (CH_{ar}), 119.0 (CH_{ar}), 119.9 (CH_{ar}), 123.3 (C_q), 126.3 (2 CH_{ar}), 126.9 (CH_{ar}), 128.6 (C_q), 130.8 (CH_{ar}), 131.0 (CH_{ar}), 134.4 (CH_{ar}), 138.6 (CH_{ar}), 139.6 (C_q), 140.9 (C_q), 147.7 (C_q), 154.1 (C_q) ppm. MS (ESI^+): *m/z* (%) = 489 (100) $[M]^+$. $C_{29}H_{34}ClN_3O_4{\cdot}0.5H_2O$ (533.06): calcd. C 65.34, H 6.62, N 7.88; found C 65.53, H 6.57, N 7.95.

Supporting Information (see footnote on the first page of this article): ^1H and ^{13}C NMR spectra of all new compounds, spectra of photometric titrations, and Job plot.

Acknowledgments

Generous support by the Deutsche Forschungsgemeinschaft is gratefully acknowledged.

[1] a) H. H. Harris, I. J. Pickering, G. N. George, *Science* **2003**, *301*, 1203; b) N. Basu, A. Scheuhammer, N. Grochowina, K. Klenavic, D. Evans, M. O Brien, M. Chan, *Environ. Sci. Technol.* **2005**, *39*, 3585; c) S. Dobson, *Cadmium: Environmental Aspects*, World Health Organization, Geneva, **1992**; d) H. L. Needleman, *Human Lead Exposure*, CRC Press, Boca Raton, FL, **1992**.

[2] S. J. Lippard, J. M. Berg, *Principles of Bioinorganic Chemistry*, University Science Books, Mill Valley, California, USA, **1994**.

[3] a) B. Valeur, *Molecular Fluorescence: Principles and Applications*, Wiley-VCH, Weinheim, **2002**; b) A. P. de Silva, H. Q. N. Gunaratne, T. Gunnlaugsson, A. J. M. Huxley, C. P. McCoy, J. T. Rademacher, T. E. Rice, *Chem. Rev.* **1997**, *97*, 1515; c) *Chemosensors of Ion and Molecule Recognition* (Eds.: J. P. Desvergne, A. W. Czarnik), Kluwer, Dordrecht, **1997**; d) B. Valeur, I. Leray, *Coord. Chem. Rev.* **2000**, *205*, 3.

[4] a) M. Zhu, M. Yuan, X. Liu, J. Xu, J. Lv, C. Huang, H. Liu, Y. Li, S. Wang, D. Zhu, *Org. Lett.* **2008**, *10*, 1481; b) R. Sheng, P. Wang, Y. Gao, Y. Wu, W. Liu, J. Ma, H. Li, S. Wu, *Org. Lett.* **2008**, *10*, 5015; c) E. Ballesteros, D. Moreno, T. Gomez, T. Rodriguez, J. Rojo, M. Garcia-Valverde, T. Torroba, *Org. Lett.* **2009**, *11*, 1269; d) S. Basurto, D. Miguel, D. Moreno, A. G. Neo, R. Quesada, T. Torroba, *Org. Biomol. Chem.* **2010**, *8*, 552; e) V. I. Minkin, A. D. Dubonosov, V. A. Bren, A. V. Tsukanov, *ARKIVOC* **2008**, *4*, 90; f) E. V. Tulyakova, O. A. Fedorova, Y. V. Fedorov, G. Jonusauskas, L. G. Kuźmina, J. A. K. Howard, A. V. Anisimov, *Russ. Chem. Bull. Int. Ed.* **2007**, *56*, 513.

[5] a) H. Yao, T. Isohashi, K. Kimura, *J. Phys. Chem. B* **2007**, *111*, 7176; b) H.-J. Xu, G.-X. Xiong, *J. Photoch. Photobiology A* **1995**, *92*, 35; c) J. V. Ros-Lis, R. Martinez-Manez, K. Rurack, F. Sancenon, J. Soto, M. Spieles, *Inorg. Chem.* **2004**, *43*, 5183.

[6] a) S. Talay, P. Gavina, E. Coronado, E. Palomares, *Org. Lett.* **2006**, *8*, 3857; b) D. Ray, P. K. Bharadwaj, *Inorg. Chem.* **2008**, *47*, 2252.

[7] a) H. N. Kim, M. H. Lee, H. J. Kim, J. S. Kim, J. Yoon, *Chem. Soc. Rev.* **2008**, *37*, 1465; b) D. T. Quang, J. S. Kim, *Chem. Rev.* **2010**, *110*, 6280.

[8] a) L. Antonov, V. Deneva, S. Simeonov, V. Kurteva, D. Nedeltcheva, J. Wirz, *Angew. Chem. Int. Ed.* **2009**, *48*, 7875; b) L. M. Antonov, V. B. Kurteva, S. P. Simeonov, V. V. Deneva, A. Crochet, K. M. Fromm, *Tetrahedron* **2010**, *66*, 4292.

[9] a) A. H. Stern, R. J. M. Hudson, C. W. Shade, S. Ekino, T. Ninomiya, M. Susa, H. H. Harris, I. J. Pickering, G. N. George, *Science* **2004**, *303*, 763; b) M. J. Scoullos, G. H. Vonkeman, L. Thornton, Z. Makuch, *Mercury, Cadmium, Lead: Handbook for Sustainable Heavy Metals Policy and Regulation (Environment & Policy, V. 31)*, Kluwer, Dordrecht, **2001**; c) T. W. Clarkson, L. Magos, G. J. Myers, *N. Engl. J. Med.* **2003**, *349*, 1731.

[10] a) M. Tian, H. Ihmels, K. Benner, *Chem. Commun.* **2010**, *46*, 5719; b) M. Tian, H. Ihmels, *Chem. Commun.* **2009**, 3175.

[11] a) A. Granzhan, H. Ihmels, *ARKIVOC* **2007**, *3*, 136; b) J. W. Sibert, P. B. Forshee, *Inorg. Chem.* **2002**, *41*, 5928.

[12] J. W. Steed, J. L. Atwood, *Supramolecular Chemistry*, 2nd ed., Wiley, Chichester, **2009**, chapter 3.

[13] J.-S. Yang, C.-Y. Hwang, C.-C. Hsieh, S.-Y. Chiou, *J. Org. Chem.* **2004**, *69*, 719.

[14] A. Granzhan, H. Ihmels, G. Viola, *J. Am. Chem. Soc.* **2007**, *129*, 1254.

[15] a) S. A. Jonker, S. Van Dijk, K. Goubitz, C. A. Reiss, W. Schuddeboom, J. W. Verhoeven, *Mol. Cryst. Liq. Cryst.* **1990**, *183*, 213; b) H. W. Mbatia, D. P. Kennedy, C. E. Camire, C. D. Incarvito, S. C. Burdette, *Eur. J. Inorg. Chem.* **2010**, 5069.

[16] J. W. Sibert, P. B. Forshee, G. R. Hundt, A. L. Sargent, S. G. Bott, V. Lynch, *Inorg. Chem.* **2007**, *46*, 10913.

[17] a) Z. Xu, K.-H. Baek, H. N. Kim, J. Cui, X. Qian, D. R. Spring, I. Shin, J. Yoon, *J. Am. Chem. Soc.* **2010**, *132*, 601; b) S. Goswami, D. Sen, N. K. Das, *Org. Lett.* **2010**, *12*, 856; c) J. Huang, Y. Xu, X. Qian, *Org. Biomol. Chem.* **2009**, *7*, 1299; d) L. Xue, C. Liu, H. Jiang, *Org. Lett.* **2009**, *11*, 1655; e) J. Huang, Y. Xu, X. Qian, *Dalton Trans.* **2009**, 1761–1766; f) C. Lu, Z. Xu, J. Cui, R. Zhang, X. Qian, *J. Org. Chem.* **2007**, *72*, 3554; g) I. H. Leubner, *J. Org. Chem.* **1973**, *38*, 1098; h) S. Arai, H. Arai, M. Hida, T. Yamagishi, *Heterocycles* **1994**, *38*, 2449.

[18] A. Y. Freidzon, A. A. Bagatur'yants, S. P. Gromov, M. V. Alfimov, *Russ. Chem. Bull. Int. Ed.* **2003**, *52*, 2646.

[19] S. F. Nelsen, E. L. Clennan, L. Echegoyan, L. A. Grezzo, *J. Org. Chem.* **1978**, *43*, 2621.

[20] B. S. Berlett, R. L. Levine, E. R. Stadtman, *Anal. Biochem.* **2000**, *287*, 329.

[21] a) M. Schmittel, H.-W. Lin, *Inorg. Chem.* **2007**, *46*, 9139; b) A. Coskun, E. U. Akkaya, *J. Am. Chem. Soc.* **2006**, *128*, 14474.

[22] H. Sakamoto, J. Ishikawa, S. Nakao, H. Wada, *Chem. Commun.* **2000**, 2395.

[23] a) G. Farruggia, S. Iotti, L. Prodi, M. Montalti, N. Zaccheroni, P. B. Savage, V. Trapani, P. Sale, F. I. Wolf, *J. Am. Chem. Soc.* **2006**, *128*, 344; b) H. Hama, T. Morozumi, H. Nakamura, *Tetrahedron Lett.* **2007**, *48*, 1859.

[24] W. Clegg, F. J. Craig, K. W. Henderson, A. R. Kennedy, R. E. Mulvey, P. A. O'Neil, D. Reed, *Inorg. Chem.* **1997**, *36*, 6238.

[25] E. M. Nolan, S. J. Lippard, *Chem. Rev.* **2008**, *108*, 3443.

[26] a) C. K. Bradsher, J. P. Sherer, J. H. Parham, *J. Chem. Eng. Data* **1965**, *10*, 180; b) M. Tanaka, M. Nakamura, T. Ikeda, K. Ikeda, H. Ando, Y. Shibutani, S. Yajima, K. Kimura, *J. Org. Chem.* **2001**, *66*, 7008.

Received: March 8, 2011
Published Online: May 27, 2011

